narrower (Table I) so that the separation of energy sublevels along the y-direction is increased. This increases the oscillation period when measuring the conductances as functions of the Fermi energy. On the other hand, the increase of the Fermi energy as a function of the lower gate bias is very significant. In the final conductances versus lower gate bias diagram, Fig. 2, the Fermi energy factor dominates, and the oscillation period in the conductance increases, as indicated in the experiments when the upper gate bias is decreased.

The calculated oscillation period increases with increasing lower gate bias in Fig. 2. This is due to the square-well approximation in the y-direction used in the model calculation. When parabolic well is used, the energy separations between sublevels are constant, so becomes the oscillation period. Thus, when real band profile is used in the transport calculation, constant oscillation period is expected.

IV. Discussion And Summary

To briefly estimate the Coulomb blockade effect, we assume a charge Q distributed uniformly in a spherical volume of radius a. The potential thus induced is given by

$$V = \frac{Q}{8\pi\epsilon\epsilon_0}\begin{cases}\frac{2}{r}, r > a\\ \left(3 - \frac{r^2}{a^2}\right), r \le a\end{cases}. \tag{3}$$

When $Q = e$ and $\epsilon = 13.1$ (silicon), we have $V = 1.1/a$ V at the surface of the sphere and $V = 1.65/a$ V at the center (a is in the unit of Å).

In the MOSFET under investigation, the length of the upper gate metal bar is 160 nm and open area between metal bars is 140 nm. If quantum dots are to be resulted by the combination of the lower and upper gates, their size is approximately $100 \times 100 \times 100$ nm^3. Inserting this into the above equation, Coulomb blockade effect is about 1 meV, far less than the oscillation period (about 17 meV) of the fine peaks in $\partial I_{sd}/\partial V_{lg}$—$V_{lg}$, while by our calculation presented in the last section, the oscillation period is about 20 meV.

In a brief summary we have calculated the conductance and transconductance of Matsuoka *et al.*'s dual-gate Si MOSFET as functions of the upper and lower gate voltages assuming quantum elastic ballistic transport. The geometry of the model conducting channel is determined from our three-dimensional calculation of the Schrödinger and Poisson equations.

It is shown that decreasing the upper gate bias makes the conducting channel created by the lower gate narrower so that the separation of the energy sublevels in the y -direction is increased. However, the decrease of the upper gate bias also greatly reduces the Fermi energy. The total effect of decreasing the upper gate bias is the decrease of the oscillation period in the conductance as functions of the lower gate bias. The calculated oscillation period as a function of the lower and upper gate bias explains very well the experimental data.

References

[1] Y. Fu and M. Willander, "Energy band diagram of a Si metal-oxide-semiconductor field-effect transistor," *IEEE Trans. Electron Devices,* vol. 42, p. 1522, 1995.

[2] H. Matsuoka, T. Ichiguchi, T. Yoshimura, and E. Takeda, "Coulomb blockade in the inversion layer of a Si metal-oxide-semiconductor field-effect transistor with a dual-gate structure," *Appl. Phys. Lett.,* vol. 64, p. 586, 1994.

[3] Y. Fu, S. C. Jain, M. Willander, and J. J. Loferski, "Valence band structures of heavily doped strained Ge_xSi_{1-x} layers," *J. Appl. Phys.,* vol. 74, p. 402, 1993.

[4] R. Haydock, V. Heine, and M. J. Kelly, "Electronic structure based on the local atomic environment for tight-binding bands," *J. Phys. C: Solid State Phys.,* vol. 5, p. 2845, 1972.

[5] C. S. Lent and D. J. Kirkner, "The quantum transmitting boundary method," *J. Appl. Phys.,* vol. 67, p. 6353, 1990.

[6] Y. Wang, J. Wang, and H. Guo, "Magnetoconductance of a stadium-shaped quantum dot: A finite-element method approach," *Phys. Rev. B,* vol. 49, p. 1928, 1994.

Simple Approach to Include External Resistances in the Monte Carlo Simulation of MESFET's and HEMT's

S. Babiker, A. Asenov, N. Cameron, and S. P. Beaumont

***Abstract*—The contact and external series resistances play an important role in the performance of modern 0.1–0.2-μm HEMT's. It is not possible to include these resistances directly into the Monte Carlo simulations. In this letter we describe a simple and efficient way to include the external series resistances into the Monte Carlo results of the intrinsic device simulations. Example of simulation results are given for a 0.2-μm pseudomorphic-HEMT.**

I. Introduction

In the Monte Carlo simulations of MESFET's and HEMT's [1], [2], the source and drain contacts regions are usually treated as ideal ohmic contacts with infinite generation/recombination rates. Complex procedures keep the number of super-particles and their average energy constant in those regions [3]. Such procedures do not account for the contact resistance which can modify severely the $I-V$ characteristics of the present generation pseudomorphic HEMT's and MESFET's with 0.1–0.2 μm gate length [4]. The measurement equipment, primarily designed for high-frequency measurements, often introduces additional series resistance in the measured dc $I-V$ characteristics.

In Drift-Diffusion simulations, external series resistance R_C can be introduced through the boundary conditions, modifying the potential at the contact by the voltage drop across the resistance R_C [5], [6]. It is difficult to apply a similar procedure in the Monte Carlo simulations due to the stochastic nature of the instantaneous contact current. Thus the results obtained from Monte Carlo simulations will correspond to an ideal "intrinsic" device which makes it difficult to directly compare the Monte Carlo simulated characteristics with real device measurements and hence to calibrate the Monte Carlo simulators. In the few published papers where Monte Carlo simulation results are directly compared to real HEMT measurements [7] there is no indication that the external to the simulation series resistances have been included which makes the comparison questionable.

In this brief, we describe a simple "post processor" approach to incorporate the contact and probes resistances in the Monte Carlo simulated $I-V$ characteristics of "intrinsic" compound FET's. The approach is illustrated in comparison between the Monte Carlo

Manuscript received January 23, 1996; revised May 28, 1996. The review of this brief was arranged by A. H. Marshak. This work was supported by EPSRC under Grant GR/J90718.

The authors are with the Nanoelectronics Research Centre, University of Glasgow, Glasgow G12 8QQ, U.K.

Publisher Item Identifier S 0018-9383(96)07746-5.

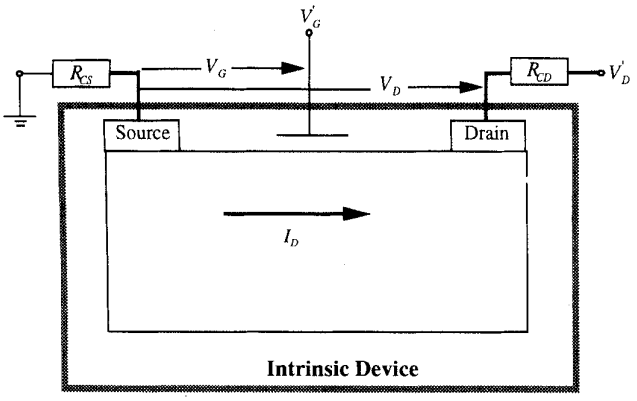

Fig. 1. The contact resistance and the measurement equipment resistance at the source and drain sides modeled as two resistances in series with the intrinsic device.

simulated and the measured characteristics of 0.2-μm pseudomorphic HEMT's fabricated in the Nanoelectronics Research Center at Glasgow University. The "extrinsic" series resistances have dramatic effect on the dc device characteristics of short-channel HEMT's and only their inclusion allows proper comparison and calibration of the simulation results.

II. The Method

Let $S = \{(V_D, V_G, I_D)\}$ be the set of all points of the I–V characteristic obtained from the Monte Carlo simulation of a particular FET, where V_D and V_G are the simulation drain and gate voltages, respectively, when the source is the reference electrode (see Fig. 1). The effect of this external to the Monte Carlo simulation resistances can be introduced as a correction to the original set of simulation data. Let us define a new set of I–V data $S' = \{(V'_D, V'_G, I_D)\}$ where V'_D and V'_G are the corrected drain and gate potentials required to maintain the same drain current through the device when the external to the simulation resistances R_{CS} and R_{CD} are taken into account. These resistances include the contact resistance and the measurement equipment resistance at the source and drain sides of the device and are obtained from independent measurements. The two sets S and S' are related by the mapping

$$V'_D = V_D + I_D(R_{CD} + R_{CS}) \quad \text{(1a)}$$

$$V'_G = V_G + I_D R_{CS}. \quad \text{(1b)}$$

The resistance of the gate Schottky contact is assumed to be infinitely high and the dc gate current is ignored. The transformation defined by (1a) and (1b) ensures that the intrinsic device characteristics remain unchanged. The set S' completely defines simulated I–V characteristics in which the effect of the external series resistances is included and can be compared to the measured characteristics of the real device. However, the raw data of S' is quite unattractive for graphical representation because the elements of the set are now a group of scattered points in the current and voltages domain. In order to compare this transformed characteristics with experimental results, we need to extract the currents for sets V_D and V_G values which correspond to the measurements and are not necessarily found in S'. Nonlinear interpolation techniques can be used to generate the modified I–V characteristics from S'. In the example results shown below a bispline interpolation provided by the contouring facility of the software GNUPLOT was used to select and plot the necessary points of the simulated and transformed I–V characteristics.

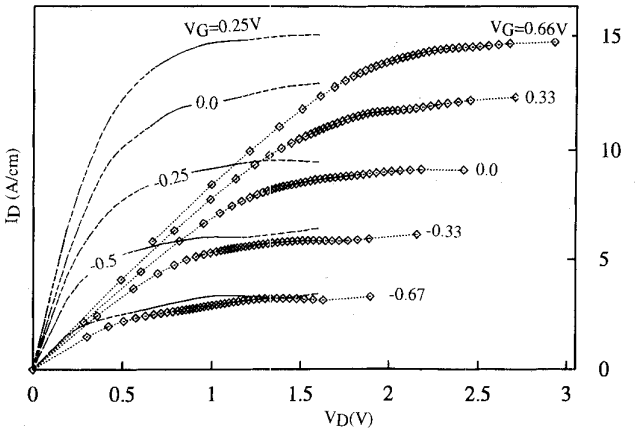

Fig. 2. The (intrinsic) I–V characteristics of a 0.2 μm p-HEMT obtained from the Monte Carlo module (lines) together with the modified I–V curves (squares) using the procedure described in the text.

III. Results

To illustrate our approach, we compare simulation results of the Monte Carlo module [7] incorporated in our **H**eterojunction **2**-D **F**inite Element FET simulator (H2F) [8] to the measured characteristics of real devices. (H2F) combines the precise finite element description of the device geometry with accurate Monte Carlo transport simulation. The multilayer problem is carefully considered in our program. In the source and drain contact regions each layer of the vertical HEMT structure is treated as an individual ohmic contact and the number of particles in each sub-region is kept constant throughout the simulation.

As an example we consider a 0.2-μm gate length recessed T-gate pseudomorphic HEMT with zero gate offset, see [9]. The zero gate offset eliminates the uncertainties related to the surface conditions in the recess region. The overall series resistance has contributions from the intrinsic device, the ohmic contacts, and the measurement equipment. It can be extracted from the linear part of the I_D–V_D characteristics at large gate voltages when the resistance of the channel is negligible [10], and was found to be 12.38 Ω for a 100-μm wide HEMT. The series resistances introduced to the source and the drain by the measurement equipment were measured by probing a short with three probes and found to be 0.2 and 2.78 Ω, respectively. The series resistance of the intrinsic device was estimated from Monte Carlo simulated I_D–V_G characteristics at low drain voltages and estimated to be 3.2 Ω. We assume that the source and drain contacts are identical and therefore each will have a series resistance of 3.1Ω. Thus the external to the Monte Carlo simulation series resistances are $R_{CS} = 0.2 + 3.1 = 3.3\,\Omega$ and $R_{CD} = 2.78 + 3.1 = 5.88\,\Omega$, respectively.

The results of the mapping and interpolation procedures are shown also in Fig. 2 together with the original results. Fig. 3 shows the calculated I_D–V_D curves at $V_G = 0$ V before and after the transformation together with the measured curve at the same gate voltage. An excellent agreement was achieved between the transformed characteristics and the experimental data in the linear region. In the saturation region our results are about 10% higher than the measurements compared to 100% difference between the simulations and the experimental data in all regions before the transformation. The 10% discrepancy can be attributed to the simplified band structure and the quantum effects that are not included in the Monte Carlo simulation.

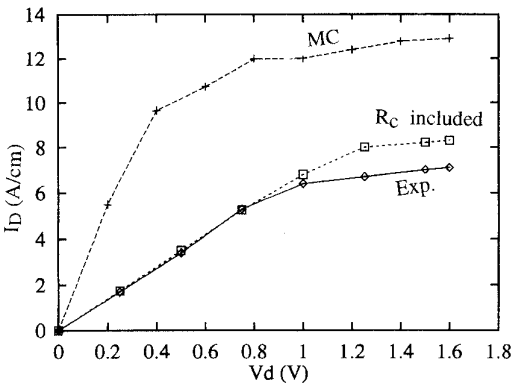

Fig. 3. The $I-V$ curves for the p-HEMT at $V_G = 0$ V: the raw data obtained from the MC module, the data corrected by including the contact, and series resistance as described in the text and the experimental data.

The contact resistance of 0.31 Ω.mm extracted for this device partially compensates for the relatively higher low-field mobility of the "intrinsic device" typical for Monte Carlo simulations of such devices. Alloy scattering, remote impurity scattering, and electron-electron scattering mechanisms are not included in our Monte Carlo simulator. The effects of the series resistance noticeable from the characteristics are: the current falls down, the transconductance is reduced, and the knee voltage shifts to higher drain voltages. The only positive effect is the slight reduction in the dc output conductance.

IV. Conclusion

In this letter, we have described a simple but effective approach to include the external series resistances in the MC simulation of compound FET's. The series resistances have profound effects on the short gate device characteristics where the channel resistances becomes comparable or even smaller than the parasitic resistances related to the cap region, the contacts, and the measurement equipment. Our approach brings to a close agreement the Monte Carlo simulation results and the experimental measurements of real short gate devices, which allows proper calibration of our Monte Carlo simulator. The results also clearly point out that very low source and drain contact and series resistances are required to benefit from the performance potential of short-channel HEMT's.

References

[1] C. Moglestue, *Monte Carlo Simulation of Semiconductor Devices.* London, U.K.: Chapman & Hall, 1993.

[2] Y. Kwon, D. Pavlidis, T. Brock, and D. Streit, "Experimental and theoretical characterization of high-performance pseudomorphic double heterojunction InAlAs/InGaAs/InAlAs HEMT's," *IEEE Trans. Electron Devices,* vol. 42, no. 6, pp. 1017–1025, 1995.

[3] D. Woolard, H. Tian, M. Littlejohn, and K. Kim, "Efficient ohmic boundary conditions for the Monte Carlo simulation of electron transport," *IEEE Trans. Electron Devices,* vol. 41, no. 4, pp. 601–606, 1994.

[4] S. Babiker, N. Cameron, A. Asenov, and S. P. Beaumont, "New evidence for velocity overshoot in a 200-nm pseudomorphic HEMT," in *Proc. ESSDERC'95,* 1995, pp. 173–176.

[5] M. Pinto, C. Raffertry, H. Yeager, and R. Dutton, "PISCES-II user's guide and supplementary report," Stanford Electronics Lab., Stanford University, CA, 1985.

[6] A. Asenov, D. Reid, J. R. Barker, N. Cameron, and S. P. Beaumont, "Finite element simulation of recess gate MESFET's and HEMT's. The Simulator H2F," in *Simulation of Semiconductor Devices and Processes,* S. Selberherr, H. Stippel, and E. Strasser, Eds. Wien: Springer-Verlag, 1993, vol. 5, pp. 265–268.

[7] S. Babiker, A. Asenov, J. R. Barker, and S. P. Beaumont, "Finite element Monte Carlo simulation of recess gate compound FET's," *Solid-State Electron.,* vol. 39, no. 5, pp. 629–635, 1996.

[8] A. Asenov, D. Reid, J. R. Barker, N. Cameron, and S. P. Beaumont, in *Simulation of Semiconductor Devices and Processes,* S. Selberherr, H. Stippel, and E. Strasser, Eds. Wien: Springer-Verlag, 1993, pp. 265–268.

[9] N. Cameron, M. Taylor, H. McLelland, M. Holland, I. Thane, K. Elgaid, and S. P. Beaumont, "A high-performance, high-yield, dry-etched pseudomorphic HEMT for W-band use," in *Proc. IEEE Microwave Theory and Tech. Symp. Dig.,* Orlando, FL, 1995, pp. 435–439.

[10] A. Raychaudhuri, J. Kolk, M. Deen, and M. King, "A simple method to extract the asymmetry in parasitic source and drain resistances from measurements on MOS transistors," *IEEE Trans. Electron Dev.,* vol. 42, no. 7, pp. 1388–1390, 1995.

Comparisons and Extension of Recent Surface Potential Models for Fully Depleted Short-Channel SOI MOSFET's

G. F. Niu, R. M. M. Chen, and G. Ruan

***Abstract*— Recent surface potential models published in this Transactions for fully depleted short-channel SOI MOSFET's are compared. The parabolic potential approach is clarified to be a special case of the quasi-2-D approach. An extended quasi-2-D model is also derived.**

I. Introduction

Fully depleted SOI MOSFET has generated substantial research interest because of its many advantages over its bulk counterpart [1]. Several surface potential models have been reported to study the short channel effects [2]–[10]. These models can be categorized into two classes: 1) solving the 2-D Poisson's equation in both silicon film and oxides using variable separation [2] or three-zone Green's function techniques [3]; and 2) solving the 2-D Poisson's equation only in the silicon film with approximate boundary conditions [4]–[10]. The results from the first class models involve infinite series, thus are not suitable for technology design and circuit simulation [7] and [10]. On the other hand, the results from the second class models have simpler form and provide more physical insight, thus these models have been applied to modeling of subthreshold swing [6], [8], [9] threshold voltage [4], [10] and subthreshold current and charges in circuit simulators [7]. This paper will first compare the two approaches leading to the second class models: The parabolic potential approach [4]–[9] and the quasi-2-D approach [10], then extend the quasi-2-D approach.

Manuscript received January 24, 1996; revised June 3, 1996. The review of this brief was arranged by Editor D. P. Verret.

G. F. Niu is the Department of Electronic Engineering, City University of Hong Kong, Hong Kong. He is also with the Department of Electronic Engineering, Fudan University, Shanghai 200433, China.

R. M. M. Chen is with the Department of Electronic Engineering, City University of Hong Kong, Hong Kong.

G. Ruan is with Department of Electronic Engineering, Fudan University, Shanghai 200433, China.

Publisher Item Identifier S 0018-9383(96)07747-7.